DESIGN OF 1/48th-SCALE MODELS FOR SHIP/ROTORCRAFT INTERACTION STUDIES

Michael R. Derby
Aerospace Computing, Inc.
Moffett Field, CA 94035

Gloria K. Yamauchi
NASA Ames Research Center
Moffett Field, CA 94035

Abstract

In support of NASA and Navy sponsored research, the Army/NASA Rotorcraft Division at Ames Research Center has designed and fabricated 1/48th-scale rotorcraft models and an amphibious assault ship model. The model scale was selected primarily to accommodate testing in the Army 7- by 10-Foot Wind Tunnel at NASA Ames. In addition to ship/rotorcraft interaction studies, the models are used to investigate the aerodynamic interaction of rotorcraft with other aircraft, with large structures, and with the ground. Four rotorcraft models representing three configurations were built: a tiltrotor aircraft, a tandem rotor helicopter, and a single main rotor helicopter. The design of these models is described and example results from several test configurations are presented.

Notation

A	aircraft total rotor disk area
b	tiltrotor wingspan
c	blade chord length
C_{Mx}	aircraft roll moment coefficient, $M_x/(\rho(\Omega R)^2(\pi R^2)R)$, positive right wing down
C_T	aircraft thrust coefficient, $T/(\rho(\Omega R)^2A)$
D	rotor diameter
DW	downwind
M_x	aircraft roll moment
N	number of blades
R	rotor blade radius
s	tiltrotor wing semispan, b/2
T	aircraft total thrust
UW	upwind
x	streamwise location of UW aircraft relative to DW aircraft, positive in drag direction
y	lateral location of UW aircraft relative to DW aircraft, positive to right (pilot's view)
z	vertical location of UW aircraft relative to DW aircraft, positive up
μ	advance ratio, tunnel speed/(ΩR)
Ω	rotor rotational speed
ρ	air density
σ	rotor geometric solidity, $Nc/(\pi R)$

Introduction

The Army/NASA Rotorcraft Division at NASA Ames Research Center has initiated an experimental program to study the aerodynamic interaction of rotorcraft with other aircraft, with large structures such as buildings and ships, and with the ground. During October 2001-June 2002, a series of experiments was conducted in the Army 7- by 10-Foot Wind Tunnel at NASA Ames investigating the aforementioned scenarios. The primary experiments completed were the shipboard operations of rotorcraft and terminal area operations of tiltrotors.[1, 2] The experimental results are providing valuable guidance in determining the effect of upwind aircraft location on a downwind on-deck aircraft, characterizing the airwake of a ship, characterizing the combined ship/rotorcraft airwake, and determining safe formation flight configurations for tiltrotors in- and out-of-ground effect for terminal area operations. In addition, the database is a valuable source for validating analyses.[1]

The primary driver for the model scale selection was to accommodate the ship/rotorcraft interaction study undertaken for the Navy. A 1/48th-scale ship was determined to be the largest size that could be tested in the 7- by 10-Foot Wind Tunnel given the test section length of 15 ft and the ship yaw angle requirements. In addition, commercial plastic fuselage kits for some of the aircraft were available at 1/48th-scale thus minimizing fabrication effort and cost.

For the ship/rotorcraft and formation flight studies addressed in this paper, correctly simulating the trailed rotor wake strength and position is key. The parameters that govern the strength and position of the trailed wake are rotor thrust and forward speed, not the details of the rotor geometry. If key nondimensional parameters such as rotor thrust coefficient and advance ratio can be matched between model and full-scale results, the model scale data should provide a good representation of full-scale events. Hence, the general aerodynamic interaction characteristics should be captured using the

1/48th-scale models. Previous work at Ames using small (approximately 1/40th-scale) tiltrotor aircraft have proven the viability of using models of this size for aerodynamic investigations.[3, 4]

This paper describes the design and fabrication of the ship and rotorcraft models and the installation of the models in the wind tunnel. The different phases of the experimental program together with the testing procedures are described. Sample results are shown.

Model Description

Most of the hardware for this experimental program was designed and fabricated by NASA Ames. For the ship/rotorcraft aerodynamic study, 1/48th-scale models of an amphibious assault ship, a tiltrotor (two), a tandem rotor helicopter, and a single main rotor helicopter were designed and fabricated. The two tiltrotors were subsequently used during the terminal area operations investigations. The following sections provide details on the ship and aircraft geometries. Model mounting is also discussed.

Ship

The ship was a low fidelity, 1/48th-scale model of an LHA amphibious assault ship. The ship geometry was scaled from the shipyard drawings of an LHA; key dimensions are provided in Table 1. The radio masts, cranes, radar antennae and other smaller features were not modeled. The ship superstructure was modeled as slab sided blocks, and includes representations of the funnels. The flight deck edge and catwalks were modeled together as a single rectangular extrusion along the port and starboard sides of the ship. The hull of the model extended down to the nominal waterline. The model bow geometry was representative of the actual ship through two removable, fiberglass skinned foam panels. All other components of the ship were constructed from 1/2 inch-thick aluminum honeycomb core panels. The deck edge elevator and the aft aircraft elevator were modeled flush with the deck. The ship was split near the midpoint into forward and aft sections that bolt together, allowing easier storage and handling. Sub-components were bolted to the main structure.

The ship was mounted internally to an aluminum rail that extends nearly the entire length of the ship. The rail was mounted to linear bearings that were welded to the tunnel turntable, which provides model yaw. The linear bearings allowed longitudinal freedom for locating the ship in the tunnel. The linear bearings were equipped with brakes to lock the ship in position. The brakes were accessible through panels located on the starboard side of the hull. The aft end of the mounting rail was supported by two castering, spring loaded wheels that prevent drooping of the aft end of the ship which was cantilevered off the end of the turntable. The wheels also allowed the model to be yawed over the sloped floor of the diffuser section of the tunnel. Brush bristles, approximately 2 in long, were attached to the bottom of the ship perimeter. The brushes served as seals to prevent unwanted airflow between the ship bottom and the tunnel floor. The pliable brushes conformed to the different size gaps between the tunnel floor and ship as the ship was translated and yawed in the tunnel. Figure 1 shows the ship mounted in the wind tunnel.

Aircraft Models

Four aircraft models were fabricated, representing 3 types of aircraft: tiltrotor, tandem rotor helicopter and single main rotor helicopter. Full-scale V-22, CH-46, and CH-53E dimensions guided the designs. Key full-scale geometric properties, provided by the Navy, are shown in Table 2. The primary modeling parameters were rotor diameter, solidity, rotor-rotor position and relative tip speed. Additionally, for the tiltrotor, the rotor-wing separation was modeled accurately. All of the models used rigid hubs and had collective control only (no cyclic). The hub and control systems were commercially available radio-control (R/C) model helicopter tail-rotor assemblies. The rotor blade pitch cases were redesigned to minimize the blade root cutout. The models were mounted on 0.75-inch diameter, six-component balances.

High-power-density R/C model motors were selected with physical dimensions compatible with the scale of the models. Each aircraft used a single Astro Cobalt-40 sport motor (AstroFlight, Inc, Model #640) mounted within the aircraft to power the rotor(s). The aircraft power requirements were estimated using a figure of merit of 0.40, which is appropriate for low Reynolds number rotors (< 50,000). Gear ratios for each transmission were chosen to provide near optimum motor operation at the selected rotor rpm. Rotor rpm was selected based on the available power, with some design margin (25%) on the estimated power requirement. The most critical power requirement was for the single main rotor helicopter model. The available motor power limited the maximum tip speed of the models to approximately 33% of full-scale.

Commercially available R/C radio transmitters, receivers, speed controllers, governors and control servos were used to remotely control rotor rpm and collective pitch. Two identical DC power supplies rated for 30 Amps at 25 Volts, powered the model motors. Batteries were used to power the collective control servo motors and speed controller. Table 3 provides a summary of the physical dimensions and properties of each model aircraft.

Tiltrotor Major components of the tiltrotor model are shown in Figure 2a. The model is shown mounted on the upwind, traversing sting in Figure 2b. The motor protruded from the nose of the aircraft, and the nacelles were not modeled. The wing was made from machined aluminum. The wing sweep and dihedral were modeled. The flaperons were set at zero degrees deflection. The rotor shafts were oriented vertically; outboard cant of the rotors was not modeled. The shafts were fixed at 90 deg for helicopter mode flight. The fuselage was a 1/48th-scale plastic model by Italeri, kit #825. The landing gear was not modeled. The rotor blade planform and twist were similar to a full-scale tiltrotor blade. The rotor blade airfoils were a blend of a low Reynolds number airfoil and a tiltrotor airfoil.

The tiltrotor model used a 2-stage gear reduction. The first stage, a 1.63:1 helical transmission, was bolted directly to the motor. The second stage was a 1.19:1 right angle gearbox that also served as the balance-mounting block. The transmission output shaft supported a magnet providing a 1/rev pulse used to govern the motor speed and provide rpm. The wings were bolted to the sides of the transmission housing. The rotor driveshafts protruded beneath the lower surface of the wing. The nacelle transmissions were 1:1 RC helicopter tail rotor transmissions. The collective control linkage ran under the wing planform to servos mounted on the sides of the transmission housing. The rotor hubs were rigid with remote control of collective pitch only. Hence the rotors operated with some non-zero hub moment in helicopter mode forward flight. Differential collective pitch could be introduced to trim rolling moment. The balance moment center was located mid-way between the two rotors in the rotor-rotor plane.

Tandem Rotor Helicopter The tandem helicopter major components are shown in Figure 3a. Figure 3b shows the model mounted on the upwind, traversing sting. The relative height and shaft angles of the rotor hubs were modeled correctly. The aft transmission was higher than the forward transmission, and the forward transmission was canted 2.50 degrees forward. The main transmission provided direct coupling to the forward transmission and a 1:1 ratio to the aft transmission. The helicopter transmission ratio was set at 1:1 in order to reduce the complexity and size of the gearbox. Although this did not provide the optimum motor rpm, the power required was still well within the power capability of the motor. A six-component balance was located under the aft rotor.

The rotor blade planform and twist were similar to the equivalent full-scale blade. A low Reynolds number airfoil was used instead of the full-scale airfoil.

A removable skin was fashioned for the model to accommodate protrusions in the body contour due to the chassis. The skin was made from 0.020-inch plastic sheet shaped to provide a more realistic profile. The skin included stub wings and the lower portion of the rear pylon and was wrapped over the chassis top and sides and secured to the chassis using Velcro strips.

Single Main Rotor Helicopter Figure 4a shows the major components of the single main rotor helicopter. Figure 4b shows the model installed on the upwind, traversing sting; the ship is seen in the background. Since a 7-bladed hub was not commercially available, a 5-bladed hub was used. The intent was to match the full-scale CH-53E (7-bladed hub) solidity. The blades were fabricated assuming an identical root cutout as the 3-bladed tandem rotor hub. Unfortunately, the root cutout of the 5-bladed hub proved to be larger; hence, the rotor radius was closer to 1/46th-scale than 1/48th. The low Reynolds number airfoil used for the tandem rotor helicopter was also used for the single main rotor helicopter blade. The blade planform and twist were representative of the full-scale helicopter. The helicopter was designed with a two-stage 4:1 gear reduction.

A 1/48th-scale plastic model kit of a CH-53G (Revell Germany) was modified to serve as the fuselage. Cut-outs were made in the kit fuselage as appropriate to ensure a snug fit around the model chassis. As shown in Fig. 4, the motor protruded from the front of the fuselage. The fuselage was secured to the chassis using small hex screws. The kit's stub wings, external auxiliary tanks, and cowling were modified to simulate the planform area of the 3-engined CH-53 variant. The tail assembly was not modeled in order to provide clearance for the sting mount.

Aircraft Mounting

For the ship/rotorcraft aerodynamic interaction study, a tiltrotor was mounted to a ship-supported sting that was manually adjustable axially, in yaw, and in height above deck. The sting was bolted to a hard point beneath the deck in the interior of the ship, thus minimizing protrusions above deck. The tiltrotor was fixed at a height corresponding to wheels on-deck full-scale. Two mounting positions were provided for the sting near the port edge of the ship, downstream of the superstructure. To simulate an aircraft operating upwind of the on-deck tiltrotor, a second aircraft (tandem rotor helicopter, single main rotor helicopter or tiltrotor) was sting-mounted and suspended from a streamlined strut attached to the tunnel traverse system. A two-piece sting was used to offset the models vertically and horizontally from the traverse. The horizontal sting could be manually yawed in fixed increments of 5 degrees up to 15 degrees (to starboard).

The upwind model could be traversed in the lateral, vertical, and streamwise directions.

For the formation flight studies, the downwind or following aircraft was mounted on a fixed pedestal mount. The mount permitted manual adjustment of model yaw, pitch, and height.

Aircraft Force and Moment Measurements

A maximum of two aircraft were tested simultaneously. Each aircraft was mounted on a six-component (5 forces, 1 moment), 0.75-inch diameter internal balance. The six components were comprised of two normal force elements providing normal force and pitching moment, two side force elements providing side force and yaw moment, an axial force element pair, and a roll moment element pair. Table 4 provides the maximum allowable load for each component.

Both balances were calibrated in the laboratory immediately before they were installed in the aircraft. For each balance, the calibration consisted of 12 single-component loading runs. The data from the 12 runs were then used to compute a calibration matrix for the balance. The normal force and rolling moment responses were accurate within approximately 0.5% of the applied load.

Results

Example results from the ship/rotorcraft interaction test and the tiltrotor formation flight test are presented. The procedures for the different test configurations are also discussed.

Ship/Rotorcraft Interaction Studies

One of the objectives of this interaction study was to characterize the airwake of the ship alone. These data could then be used to validate analyses without the added complexity of including the effects of one or more rotorcraft. Some limited surface flow visualization was acquired by applying an oil mixture to the surface of the ship deck. The oil mixture consisted of motor oil, olive oil, mineral spirits, and titanium dioxide. Figure 5 shows the resulting oil pattern for a yaw angle of 15 deg and an approximate freestream velocity of 36 ft/s. The oil required about 20 minutes to reach a stable pattern. A line of oil build-up is seen in the figure originating from the port leading edge and extending the length of the deck. Subsequent velocity field measurements acquired using Particle Image Velocimetry (PIV) suggest the oil line represents the path of a vortex originating from the port leading edge.

PIV was used to acquire three components of velocity in a 3-ft by 6-ft (H x W) plane oriented perpendicular to the freestream. Data were acquired at 4 landing spots and four yaw angles (representing port-side winds) over a range of velocities. Figure 6 shows several planes of PIV data superimposed on the ship. The reverse flow region behind the ship superstructure is clearly shown. Vortical regions located approximately at the same location from the deck edge as the oil line in Fig. 5 are also seen.

The majority of the ship/rotorcraft interaction test concentrated on acquiring aircraft force and moment data for different arrangements of aircraft on or near the ship. Figure 7 shows the installation of the primary configuration tested: a tiltrotor on the ship deck with a tandem rotor helicopter operating upwind. The tiltrotor aircraft was set to an initial low thrust level without the influence of the upwind aircraft. The upwind aircraft was then set at a desired thrust and traversed in a pre-programmed grid in the x-y plane (Fig. 8) at a given height above deck, z, while the tiltrotor forces and moments were allowed to vary. At each position, the upwind aircraft was trimmed to the desired thrust before recording a data point. Using this procedure, the forces and moments of the on-deck tiltrotor were mapped as a function of upwind aircraft position. These mappings were acquired for several wind speeds at ship yaw angles of 0 and 15 degrees (to starboard). The test results provide guidance in establishing safe shipboard operational limits of the corresponding full-scale rotorcraft.

Formation Flight

The aerodynamic interaction of two model tiltrotors in helicopter-mode formation flight was investigated as part of the NASA Runway Independent Aircraft Program. The thrust and the roll moment of the downwind aircraft were the primary measures of the aerodynamic interaction between the two aircraft. Three scenarios representing tandem level flight, tandem operations near the ground, and a single tiltrotor operating above the ground for varying winds were examined and the results reported.[2]

Figure 9 shows the two tiltrotors installed in the Army 7- by 10-Foot Wind Tunnel. The pitch attitude of both aircraft was fixed at zero; therefore, both rotor tip-path planes were horizontal. The upwind model was traversed in the lateral, vertical, and streamwise directions upstream of the downwind stationary aircraft. Figure 10 shows the two aircraft with a ground plane installed. The ground plane is 4-ft by 8-ft and approximately 1.25 inches thick with a rounded leading edge.

Based on limited velocity field measurements acquired downstream of one of the tiltrotors (without a ground plane), it is known that a tiltrotor wake looks very much like the wake of a fixed wing aircraft. Each rotor disk is assumed to shed a counter-rotating vortex pair. Vortices shed from the inboard side of each disk are equal in magnitude but opposite in sign leading to vortex cancellation because of their close proximity. The outboard vortex from each disk remains to dominate the far wake as super-vortices. The existence of these super-vortices is also confirmed by calculation.[1] When these super-vortices approach the ground plane, they tend to migrate outward since the ground plane acts as an image plane.

Figures 11 and 12 show contours of the downwind aircraft rolling moment as a function of upwind aircraft position with and without the ground plane, respectively, for several aircraft separation distances. The initial C_T/σ of the downwind aircraft was 0.018 and the upwind aircraft was trimmed to about C_T/σ=0.12 and approximately zero roll moment. The locations where data were acquired are shown as overlaid grid points. With the ground plane present, the lowest vertical position of the upwind aircraft was limited to z/s values slightly greater than zero to prevent wiring and cooling lines, which hang below the aircraft, from touching the ground plane. Data without the ground plane (Fig. 12) are shown solely to illustrate the effects of the ground plane – the low C_T/σ of the downwind aircraft is unrealistic for level flight. With the ground plane present, the peak negative roll moment location moves outboard as x/D is varied from -2.5 to -7.5. The magnitude of the peak negative moment is somewhat mitigated by the ground plane. Interestingly, a positive peak moment is present at y/s=-1 with the ground plane. This peak positive moment is possibly caused by the super-vortex from the right upwind rotor that, instead of traveling straight downstream, has moved outward to the right under the influence of the ground plane. Without the ground plane, the lateral location of the peak rolling moment does not change with increasing separation distance indicating that the wake from the upwind aircraft convects straight downstream. Ground plane surface flow visualization images obtained using tufts and oil were used to help understand the mutual interaction between the two aircraft. With the ground plane, the downwind aircraft wake was clearly observed to influence the upwind aircraft wake trajectory.

These data provide guidance in determining tiltrotor flight formations which minimize disturbance to the trailing aircraft.

Concluding Remarks

The results from these experiments have provided significant insight into the aerodynamic interaction of rotorcraft operating in close proximity to each other and to other structures. The models have provided data which are currently being used to guide full-scale operations of rotorcraft operating on ships and in formation flight.

Acknowledgements

The authors wish to thank Jim Kennon, Dan Kalcic, and Gina Clemente of NASA Ames who contributed to the design of the aircraft mounting, the tandem rotor model, and the single main rotor model. The excellent work of the NASA Ames model shop and machine shop in fabricating the ship, aircraft models, and mounting hardware is gratefully acknowledged. The rotor blade molds were fabricated by APC Props. The rotor blades were made by Chuck Winters.

The ship/rotorcraft interaction study was funded primarily by the U.S. Navy, V-22 Program Office.

References

1. Johnson, W., Derby, M. D., Wadcock, A. J., and Yamauchi, G. K., "Wind Tunnel Measurements and Calculations of Aerodynamic Interactions Between Tiltrotor Aircraft," American Institute of Aeronautics and Astronautics, 41st Aerospace Sciences Meeting and Exhibit, Reno, NV, January 2003.

2. Yamauchi, G. K., Wadcock, A. J., and Derby, M. D., "Measured Aerodynamic Interaction Between Two Tiltrotors," American Helicopter Society 59th Annual Forum, Phoenix, AZ, May 2003.

3. Abrego, A. and Long, K., "A Wind Tunnel Investigation of a Small-Scale Tiltrotor Model in Descending Flight," American Helicopter Society Aerodynamics, Acoustics, and Test and Evaluation Technical Specialists Meeting, San Francisco, CA, January 2002.

4. Abrego, A. I., Betzina, M. D., and Long, K. R., "A Small-Scale Tiltrotor Model Operating in Descending Flight," 28th European Rotorcraft Forum, Bristol, United Kingdom, September 2002.

Table 1. Ship Properties

	Full Scale LHA	1/48th-scale model
Flight deck length	820 ft	205.0 in
Flight deck width	118.1 ft	29.53 in
Nominal height above waterline	64.5 ft	16.13 in

Table 2. Full-Scale Aircraft Properties

	V-22 Osprey	CH-46	CH-53E
No. of rotors	2	2	1
No. blades per rotor	3	3	7
Rotor radius (in)	228.5	306.0	474.0
Blade tip chord (in)	22.00	18.75	29.28
Rotor solidity	0.105*	0.059†	0.138†
Rotor RPM (100%)	397	264	177
Tip speed (ft/s)	792	705	732
Blade tip Reynolds number	9.26×10^{6}	7.03×10^{6}	11.39×10^{6}

* Thrust weighted

† Geometric

Table 3. Scale Model Aircraft Properties

	Tiltrotor	Tandem Rotor Helicopter	Single Main Rotor Helicopter
No. of rotors	2	2	1
No. blades per rotor	3	3	5
Rotor radius (in)	4.687	6.311	10.220
Blade tip chord (in)	0.446	0.375	0.854
Rotor solidity	0.102*	0.057†	0.133†
Target rotor RPM	6,355	4,224	2,831
Target tip speed (ft/s)	260	233	252
Blade tip Reynolds number	61,616	46,366	114,604
Motor design speed (rpm)	12,313	4,224	11,324
Gear ratio	1.9375	1.0	4.0
Design power, including 25% margin (W)	251	69	304

* Thrust weighted

† Geometric

Table 4. Balance Load Limits

Load Direction	Maximum Allowed Load
N1	±25.0 lb
N2	±25.0 lb
S1	±12.5 lb
S2	±12.5 lb
AX	±50.0 lb
RM	±25.0 in-lb

Figure 1. 1/48th-scale amphibious assault ship installed in Army 7- by 10-Foot Wind Tunnel at NASA Ames.

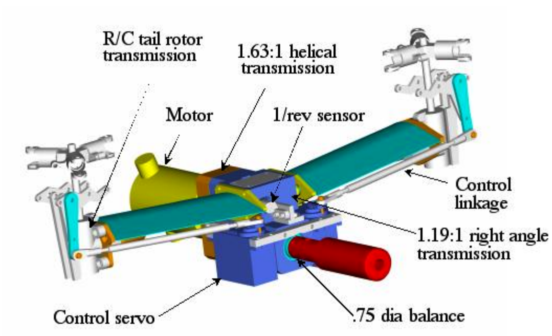

a) Tiltrotor major components.

b) Mounted on upwind sting.

Figure 2. Tiltrotor model.

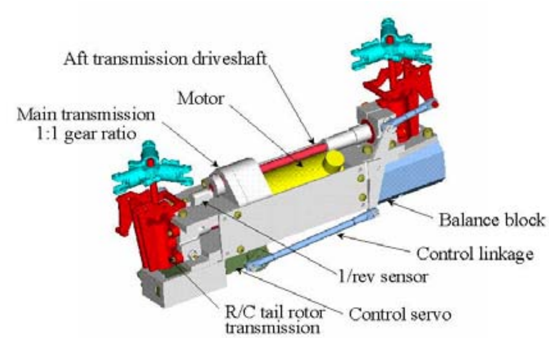

a) Tandem rotor helicopter major components.

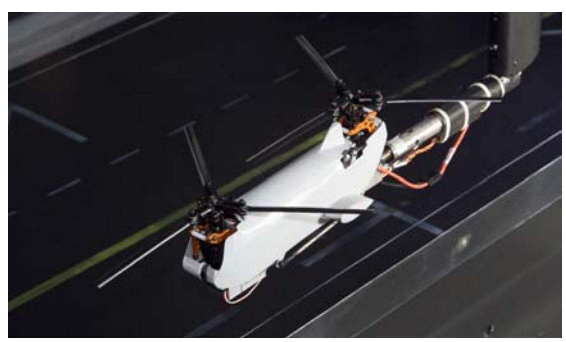

b) Mounted on upwind sting.

Figure 3. Tandem rotor helicopter.

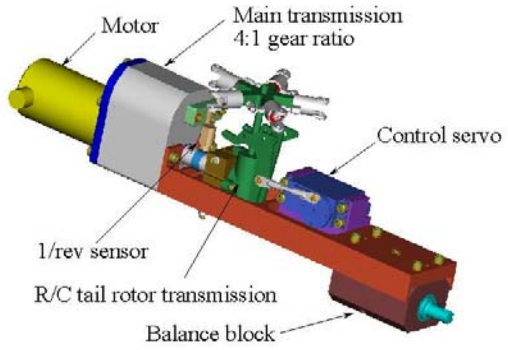

a) Single main rotor helicopter major components.

b) Helicopter mounted on upwind sting.

Figure 4. Single main rotor helicopter.

Figure 5. Surface oil flow visualization of deck for yaw = 15 deg. View from rear of ship.

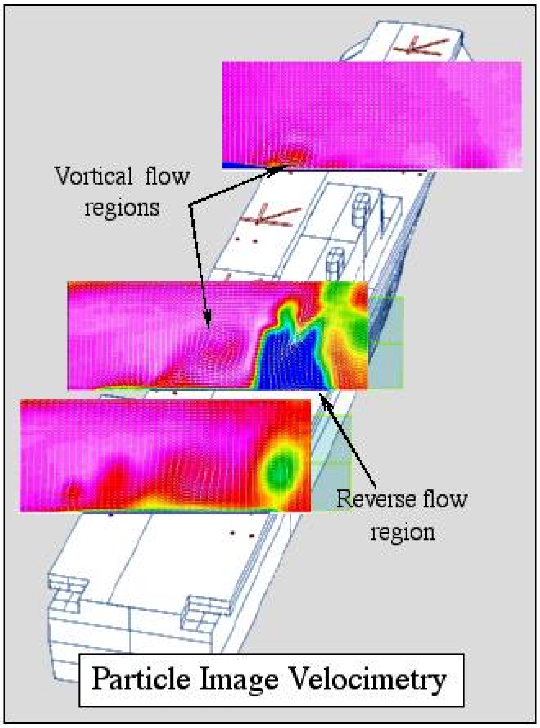

Figure 6. Velocity fields at different landing spots for yaw = 15 deg.

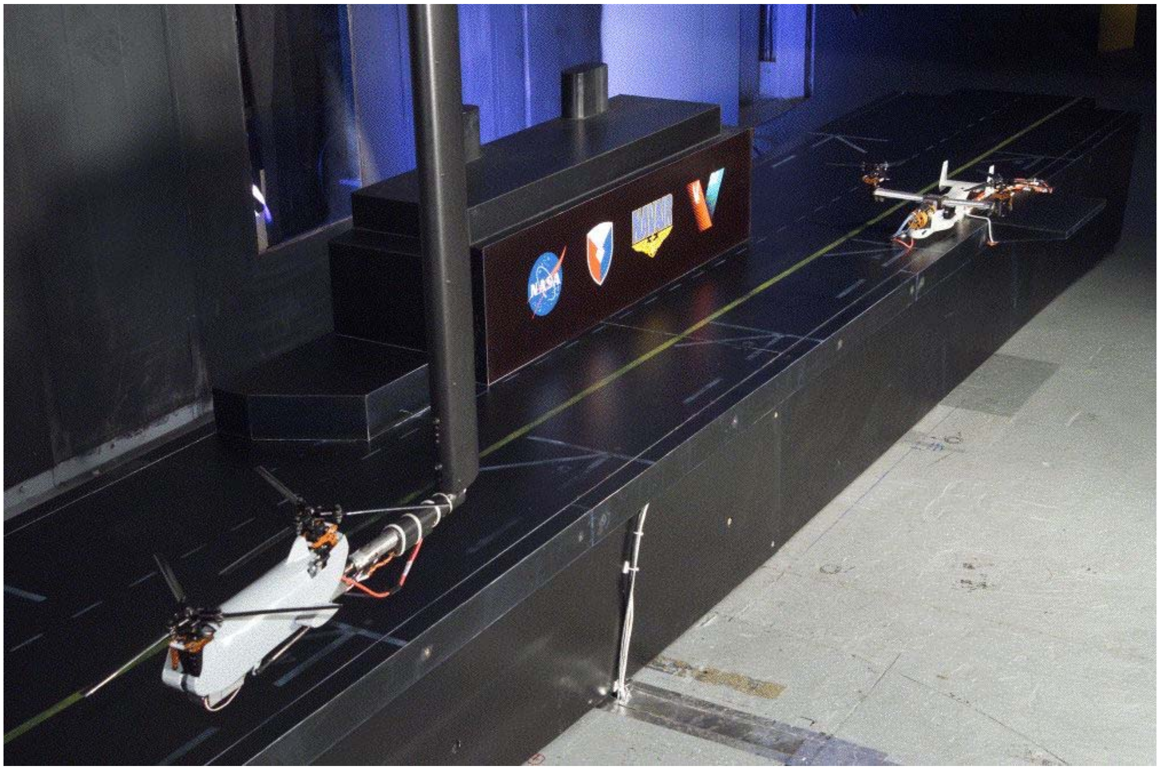

Figure 7. Installation of ship and rotorcraft in Army 7- by 10-Foot Wind Tunnel.

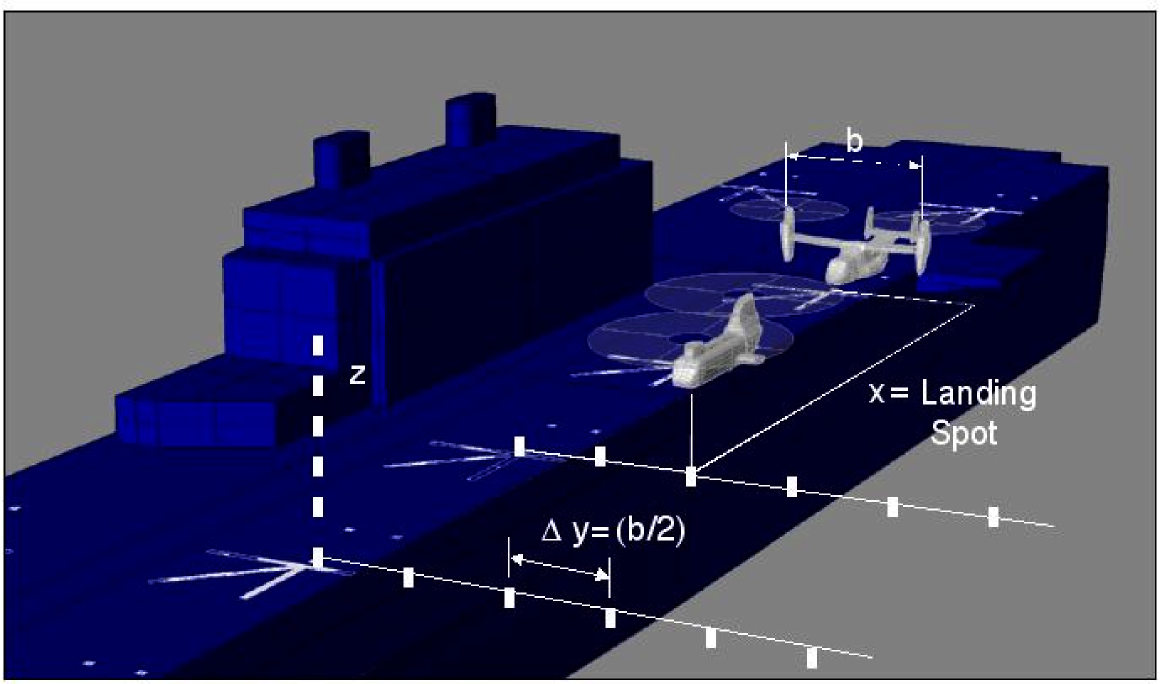

Figure 8. Geometry for mapping forces and moments of rotorcraft operating near or on the ship.

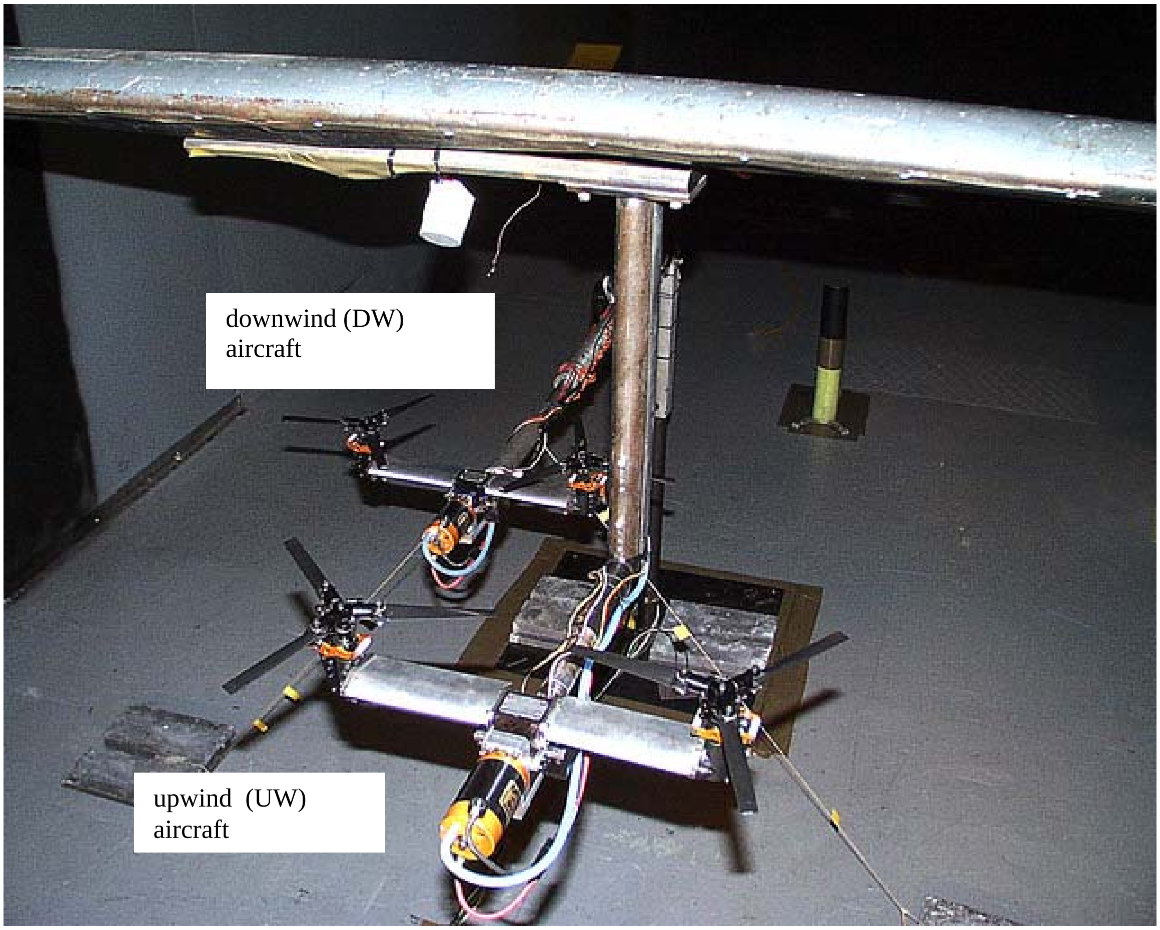

Figure 9. Tiltrotor models installed in Army 7- by 10-Foot Wind Tunnel in formation flight configuration.

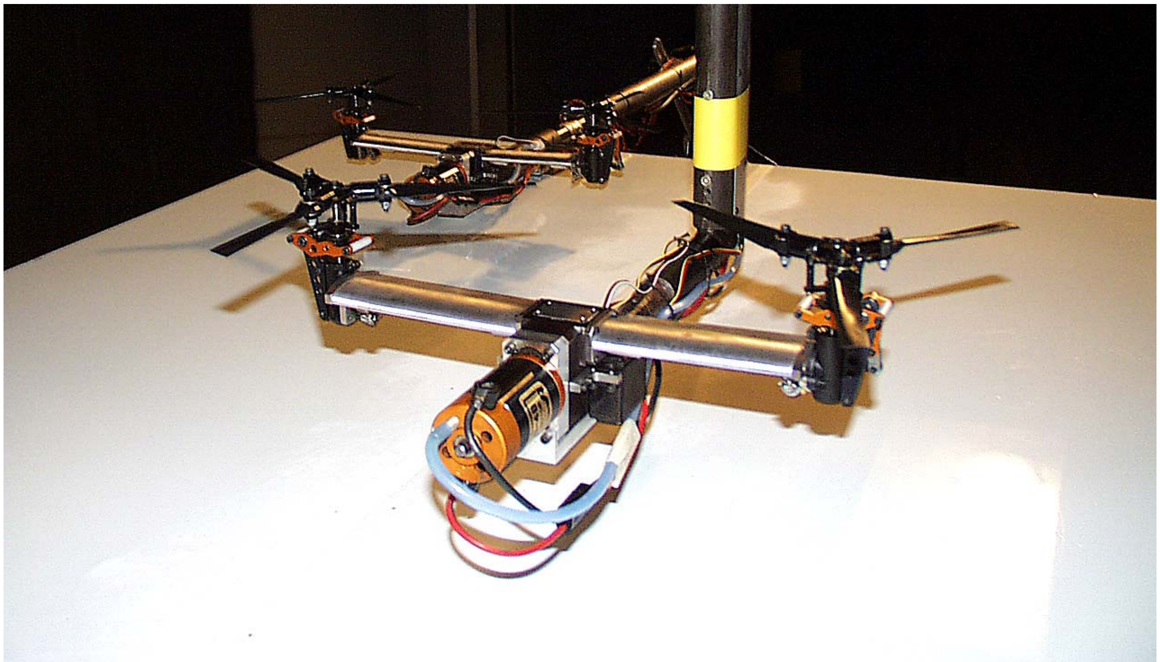

Figure 10. Tiltrotor models installed with ground plane.

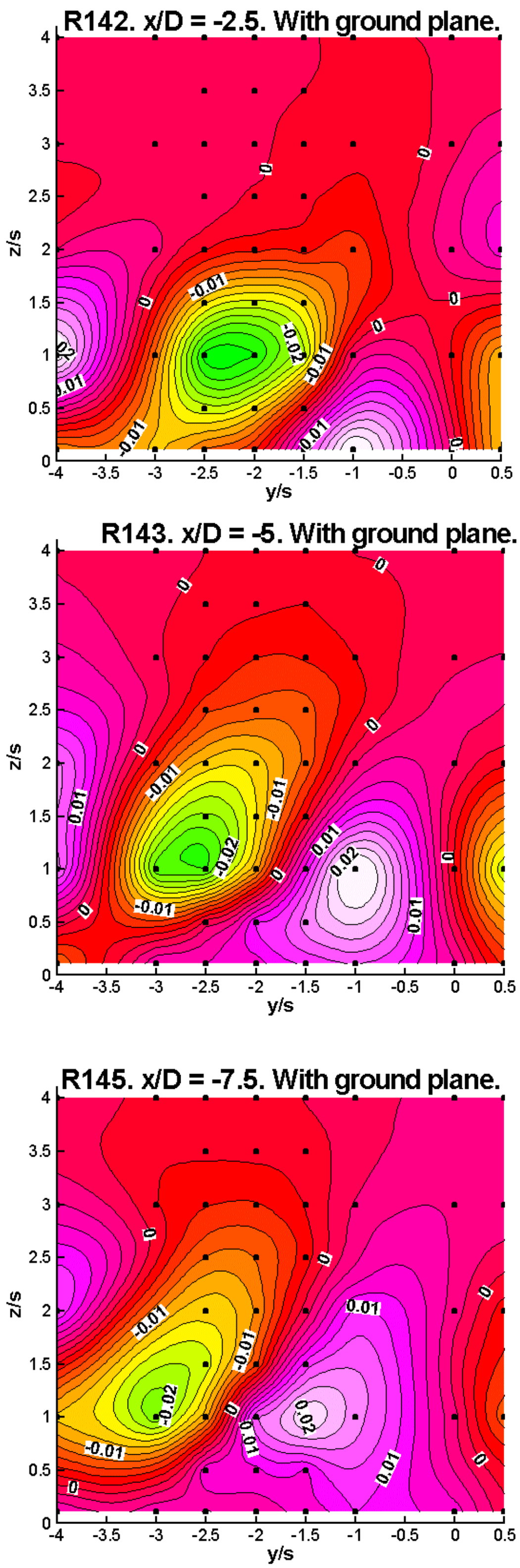

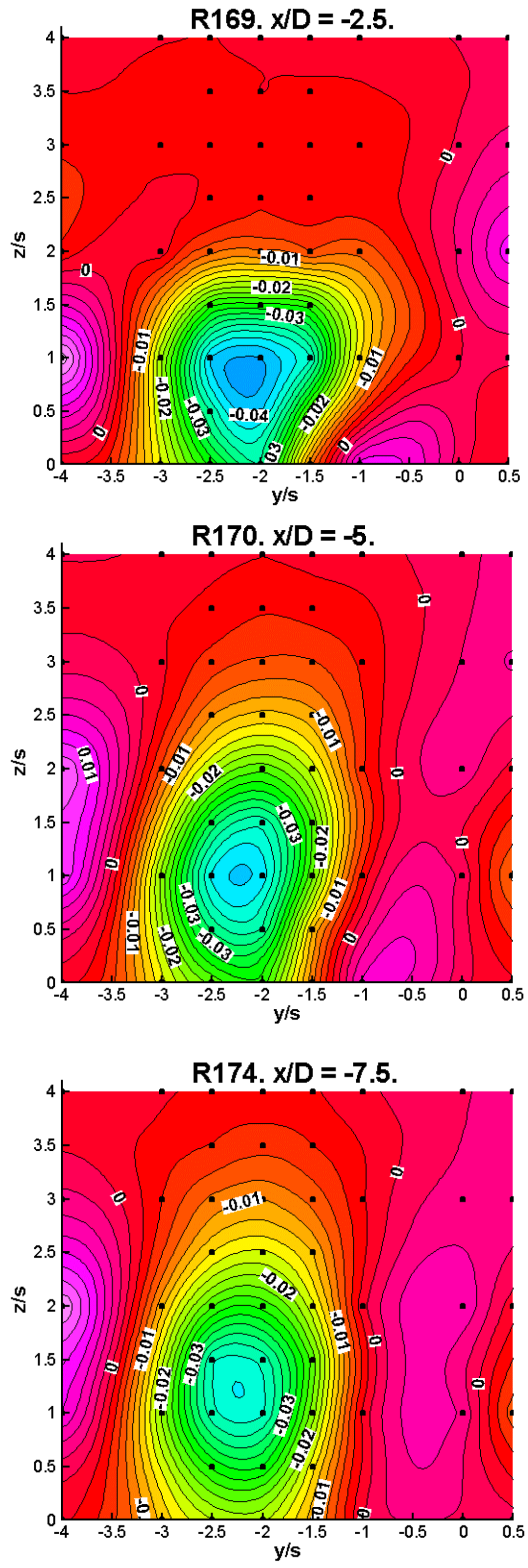

Figure 11. DW aircraft C_{Mx}/σ as a function of UW aircraft position. With ground plane. μ =0.10.
DW C_T/σ (initial)=0.018; UW C_T/σ=0.12.

Figure 12. DW aircraft C_{Mx}/σ as a function of UW aircraft position. Without ground plane. μ =0.10.
DW C_T/σ (initial)=0.018; UW C_T/σ=0.12.